Maxi K^+ Channels and Their Relationship to the Apical Membrane Conductance in *Necturus* Gallbladder Epithelium

YOAV SEGAL and LUIS REUSS

From the Department of Physiology and Biophysics, The University of Texas Medical Branch, Galveston, Texas

ABSTRACT Using the patch-clamp technique, we have identified large-conductance (maxi) K^+ channels in the apical membrane of *Necturus* gallbladder epithelium, and in dissociated gallbladder epithelial cells. These channels are more than tenfold selective for K^+ over Na^+, and exhibit unitary conductance of ~200 pS in symmetric 100 mM KCl. They are activated by elevation of internal Ca^{2+} levels and membrane depolarization. The properties of these channels could account for the previously observed voltage and Ca^{2+} sensitivities of the macroscopic apical membrane conductance (G_a). G_a was determined as a function of apical membrane voltage, using intracellular microelectrode techniques. Its value was 180 $\mu S/cm^2$ at the control membrane voltage of −68 mV, and increased steeply with membrane depolarization, reaching 650 $\mu S/cm^2$ at −25 mV. We have related maxi K^+ channel properties and G_a quantitatively, relying on the premise that at any apical membrane voltage G_a comprises a leakage conductance and a conductance due to maxi K^+ channels. Comparison between G_a and maxi K^+ channels reveals that the latter are present at a surface density of 0.09/μm^2, are open ~15% of the time under control conditions, and account for 17% of control G_a. Depolarizing the apical membrane voltage leads to a steep increase in channel steady-state open probability. When correlated with patch-clamp studies examining the Ca^{2+} and voltage dependencies of single maxi K^+ channels, results from intracellular microelectrode experiments indicate that maxi K^+ channel activity in situ is higher than predicted from the measured apical membrane voltage and estimated bulk cytosolic Ca^{2+} activity. Mechanisms that could account for this finding are proposed.

INTRODUCTION

Large-conductance (maxi) K^+ channels have been characterized in numerous excitable and nonexcitable tissues (Latorre and Miller, 1983; Latorre, 1986; Blatz and Magleby, 1987). Ion permeation and gating behavior in maxi K^+ channels have been examined in depth, and recent studies have highlighted the complexity of these processes. Maxi K^+ channels are highly K^+ selective and exhibit large (>150 pS) unitary conductances; both of these properties figure into recent models of multi-ion con-

Address reprint requests to Dr. Luis Reuss, Department of Physiology and Biophysics, The University of Texas Medical Branch, Galveston, TX 77550-2781.

J. GEN. PHYSIOL. © The Rockefeller University Press · 0022-1295/90/05/0791/28 $2.00
Volume 95 May 1990 791–818

duction in maxi K^+ channels (Eisenman et al., 1986; Neyton and Miller, 1988). Gating is governed primarily by membrane voltage and internal Ca^{2+} activity. Transitions occur among a multiplicity of open and closed states, and among qualitatively different kinetic modes (McManus and Magleby, 1988).

In excitable cells, it is clear that maxi K^+ channels are well suited to repolarize the cell membrane voltage during the action potential, as they activate in response to membrane depolarization and/or to transient increases in intracellular Ca^{2+} (Lang and Ritchie, 1987). The role of maxi K^+ channels in nonexcitable cells, including epithelial tissues, has been more difficult to ascertain. Large-conductance Ca^{2+}-activated K^+ channels are present in the apical membrane of several epithelia (for reviews see Palmer, 1986; Greger and Gögelein, 1987; Wills and Zweifach, 1987), including amphibian gallbladder (Maruyama et al., 1986). In segments of the distal tubule, maxi K^+ channels may provide a pathway for K^+ secretion, though the mechanism(s) by which channels are activated remain in question (Hunter et al., 1986; Frindt and Palmer, 1987; Guggino et al., 1987). In *Necturus* choroid plexus, maxi K^+ channels in the ventricular membrane appear to play a role in the volume regulatory decrease elicited by hyposmotic swelling (Christensen, 1987). In these and other cases, maxi K^+ channel open probability under resting conditions appears to be small (< 0.1).

In this paper, we describe maxi K^+ channels that are present in the apical membrane of *Necturus* gallbladder, and in dissociated *Necturus* gallbladder epithelial cells. Our major goal is to assess the contribution of these channels to the resting apical membrane K^+ conductance (G_a), and to the increase in G_a elicited by apical membrane depolarization (García-Díaz et al., 1983; Stoddard and Reuss, 1988*b*). We develop simple models to describe the steady-state gating and conduction properties of single maxi K^+ channels, and use these models as a basis to draw quantitative comparisons with the apical membrane conductance, assessed using intracellular microelectrode techniques.

Parts of this work have appeared in preliminary form (Segal and Reuss, 1988).

MATERIALS AND METHODS

Mudpuppies (*Necturus maculosus*) were purchased from Nasco Biologicals (Ft. Atkinson, WI) or Kon's Scientific (Germantown, WI) and kept in tap water at 5°C. The animals were anesthetized in tricaine methanesulfonate. All experiments were performed at room temperature.

Patch-Clamp Experiments

Experimental preparations. Patch-clamp studies were carried out on intact gallbladders and on dissociated gallbladder epithelial cells from *Necturus maculosus*. In experiments on the intact gallbladder, the tissue was excised and mounted as a flat sheet, apical side up, in a modified Ussing chamber, as previously described (Reuss and Finn, 1975*a*, *b*; Weinman and Reuss, 1982). In attempts to remove mucus, the apical surface of the tissue was exposed for 1 h to 1 mg/ml hyaluronidase (Sigma Type IV or V, dissolved in NaCl Ringer's solution), and then rinsed. Hyaluronidase treatment had no effects on the electrical properties of the tissue, assessed using microelectrode techniques.

To prepare suspensions of dissociated cells, gallbladders were removed, sliced open, drained of bile, and pinned apical side up in a Sylgard-coated Petri dish filled with NaCl

Ringer's. Sheets of epithelial cells were scraped from the tissue with a glass coverslip; in many cases, it was possible to remove the entire epithelial cell layer as a single sheet. Epithelial sheets were collected with a 200-μl pipettor and transferred to a 15-ml centrifuge tube, where they were bathed for 7 min in 1 mg/ml hyaluronidase. Cells were then spun down; the cell-free supernatant was aspirated from the centrifuge tube, and dissociated cells were resuspended in NaCl Ringer's. Cells were transferred to an experimental chamber (described below) positioned on the stage of an inverted microscope (Diaphot; Nikon, Garden City, NY). Dissociated cell suspensions contained spherical cells that excluded the dye trypan blue, and broken cells that did not. Dye-excluding cells could be patched; these cells comprised 5–80% of the cells in any given experimental preparation.

Solutions. Tissues or dissociated cells were initially bathed in NaCl Ringer's solution containing (in millimolar): 97.5 NaCl, 2.5 KCl, 1 $MgCl_2$, 1 $CaCl_2$, 10 *N*-2-hydroxyethylpiperazine-*N'*-2-ethanesulfonic acid (HEPES)/NaOH, pH 7.4. The patch pipette was usually filled with KCl solution containing (in millimolar): 100 KCl, 1 $MgCl_2$, 10 HEPES/KOH, pH 7.4. KCl and K gluconate solutions used in determining the ion selectivity of channels in excised patches contained (in millimolar): 100 KCl or K gluconate, 1 $CaCl_2$, 10 HEPES/KOH, pH 7.4. In inside-out patch experiments measuring *I–V* relations for channels exposed to physiologic K^+ and Na^+ concentrations, the bath contained (in millimolar): 90 KCl, 10 NaCl, 1 $CaCl_2$, 10 HEPES/KOH, pH 7.4; the pipette contained NaCl Ringer's. In studies examining the Ca^{2+} sensitivity of channels in excised patches, the bathing solutions contained (in millimolar): 100 KCl, 10 HEPES/KOH, pH 7.4, 3 ethyleneglycol-bis(β-aminoethylether)-*N,N'*-tetraacetic acid (EGTA), and sufficient $CaCl_2$ to achieve the desired free Ca^{2+} concentration (range, 0.1–1 μM), calculated using equilibrium constants from Martell and Smith (1974) and a H^+ activity coefficient of 0.78. In pilot studies, the Ca^{2+} activity of these solutions was verified using a Ca^{2+}-sensitive macroelectrode (World Precision Instruments, New Haven, CT), calibrated in the pCa range of 3–7 using commercial standards (World Precision Instruments) or the calibration solutions described by Tsien and Rink (1980).

Patch-clamp techniques. Patch pipettes were made from Corning 7052 capillary glass (1.5 mm o.d., 1.0 mm i.d.; Friedrick and Dimmock, Millville, NJ) or from hematocrit glass (blue-tip; Fisher Scientific), using a two-stage vertical puller (model PP-83; Narishige, Japan). Pipettes made from Corning 7052 glass were Sylgard-coated and fire-polished to a resistance of 7–10 MΩ. Pipettes made from hematocrit glass were Sylgard-coated and used without fire-polishing; useful pipettes had 7–10 MΩ resistances. Resistances were measured with NaCl Ringer's in the bath and 100 mM KCl solution in the pipette.

In studies on the intact epithelium, patch pipettes were lowered gently onto the apical surface of the tissue. Application of suction to the pipette interior generally resulted in the formation of an ~100-MΩ seal, and in <5% of the trials, formation of a tight (>1 GΩ) electrical seal. Here, we report results obtained with gigaseals only. Membrane patches were excised by rapidly withdrawing the pipette.

Seals in the range 10–20 GΩ were routinely achieved on dissociated cells. In these experiments, patches were excised by gently tapping the microscope stage. Vesicle formation at the pipette tip usually accompanied patch excision; vesicles were disrupted by passing the pipette tip through the bath-air interface, or by applying slight positive pressure to the pipette interior. Once excised, membrane patches were transferred from the main compartment of the chamber (2–3 ml volume) to a 0.5-ml subcompartment, where they were superfused continuously at a rate of 3–5 ml/min.

Patch currents were amplified with a List EPC-7 patch clamp and recorded at wide bandwidth (DC to 20 kHz bandwidth) on video tape, using an Indec IR-2 Digital Instrumentation Recorder (Indec Systems Inc., Sunnyvale, CA). Stored records were low-pass filtered at 1–2 kHz with an eight-pole Bessel filter (model 902LPF; Frequency Devices, Inc., Haverhill, MA), and played onto a strip chart recorder (model 220; Gould Instruments, Cleveland, OH) for

analysis by hand, or digitized at 5–10 kHz for analysis by computer. In cell-attached patch experiments, pipette potentials (V_p) are expressed with respect to the bath. In experiments on inside-out patches, holding potentials are expressed so as to correspond to the cell membrane voltage (V_m), i.e., with respect to the pipette solution. In most experiments, V_m was limited to the range ± 60 mV, since seals tended to degrade at more extreme membrane voltages. Holding potentials were corrected for liquid junction potentials which arose at the bridge-bath interface during solution changes. Positive current is deemed to flow from the cellular to the extracellular side of the patches, and is depicted as upward deflections. In all experiments, the bath was grounded with an Ag-AgCl wire immersed in a Ringer's agar bridge.

Single-channel open probabilities (P_o) were estimated using segments of digitized data 10–60 s in duration, according to $P_o = (1/N_c) \Sigma\, i\, P_i$, where i is a summation index from 0 to N_c, P_i is the fraction of time during which i channels are open, and N_c is the total number of channels in the patch. This expression assumes that channels in multiple-channel patches gate identically and independently, that is, in a binomial fashion. In compiling our results, we did not use patches in which channels deviated from binomial behavior (<20% of the total). Channel openings were detected by an amplitude-threshold technique. In some cases, records were digitally filtered at 100 Hz before analysis.

A single set of voltage-step experiments was carried out to assess the time course of maxi K^+ channel activation. These experiments were carried out using inside-out patches exposed to symmetrical 100 mM KCl solutions, with internal Ca^{2+} buffered to 500 nM. For each voltage step, 30–70 current traces were averaged to construct an ensemble current. Capacitive currents were digitally subtracted from the ensemble current, using steps during which no channels were activated.

Microelectrode Experiments

Details on electrical measurements of the transepithelial voltage (V_{ms}), and the cell membrane voltages (apical, V_{mc}; basolateral, V_{cs}) have appeared previously (Reuss and Finn, 1975*a*, *b*). Gallbladders were mounted in a modified Ussing chamber and superfused symmetrically with Ringer's containing (in millimolar): 97.5 NaCl, 2.5 KCl, 1 $MgCl_2$, 1 $CaCl_2$, 10 HEPES/NaOH, pH 7.5. Cells were impaled with microelectrodes pulled from inner-fiber borosilicate glass (1 mm o.d., 0.5 mm i.d.; Glass Company of America, Millville, NJ) and filled with 1 M KCl; tip resistances ranged from 40 to 100 MΩ.

The goal of these microelectrode experiments was to estimate the apical and basolateral membrane conductances (G_a and G_b) under control conditions and during perturbations of V_{mc} induced by transepithelial current clamps. To estimate G_a and G_b under control conditions, we carried out a series of two-electrode intraepithelial cable analysis experiments, in combination with measurements of transepithelial electrical resistance (R_t) and the apparent ratio of cell membrane resistances R_a/R_b (Frömter, 1972; Reuss and Finn, 1975*a*). Cable experiments were performed as described previously (Reuss and Finn, 1975*a*; Stoddard and Reuss, 1988*a*). Hyperpolarizing current pulses 1 s in duration and 25 nA in amplitude were injected intracellularly through one electrode, and basolateral membrane voltage deflections in nearby cells were recorded as a function of distance [$\Delta V_{cs}(x)$] with a second intracellular microelectrode. Estimates for R_t and R_a/R_b were obtained using mucosa-to-serosa current pulses 1 s in duration and 50 $\mu A/cm^2$ in amplitude; these current pulses hyperpolarized V_{mc} by < 5 mV, minimizing voltage-induced changes in G_a. Estimation of equivalent circuit parameters from two-microelectrode cable data was carried out as described previously (Frömter, 1972; Reuss and Finn, 1975*a*). Briefly, the tissue was treated as a two-dimensional cable. Experimentally determined $\Delta V_{cs}(x)$ was used to estimate R_z, which equals R_a and R_b in parallel. R_z, coupled with measurements of R_t, R_a/R_b and the cell membrane voltages, permit-

ted calculation of the resistances, R_a, R_b, and R_s, and the equivalent electromotive forces (EMFs) E_a and E_b.

In a separate set of studies, G_a was estimated as a function of V_{mc} using 1-s transepithelial current clamps in the range ± 300 $\mu A/cm^2$ (Stoddard and Reuss, 1988*b*). The ratio of cell membrane voltage deflections ($\Delta V_{mc}/\Delta V_{cs}$) was measured 800 ms after the onset of each clamp, when the voltage deflections ΔV_{mc} and ΔV_{cs} had reached stable values. By this time, channels had reached steady-state gating (see Results), permitting comparisons between microelectrode measurements and results obtained from single-channel studies. Barring changes in R_a and R_b induced by the current clamp, the ratio of the voltage deflections $\Delta V_{mc}/\Delta V_{cs}$ provides a reasonable estimate for R_a/R_b (Stoddard and Reuss, 1988*a*). Recent work has revealed that depolarizing V_{mc} decreases R_a (García-Díaz et al., 1983; Stoddard and Reuss, 1988*b*). In the Appendix, we refine the procedure for estimating R_a/R_b from $\Delta V_{mc}/\Delta V_{cs}$ measurements, accounting for voltage-induced changes in G_a and E_a.

Statistics and Curve Fitting

Experimental values are expressed as mean ± standard error of measurement (SEM). Fitting programs used a grid-search algorithm for minimizing the sum of squared deviations (Bevington, 1969).

MODELS

The basic expression relating the macroscopic apical membrane conductance $G_a(V_{mc})$ to ion channels in the apical membrane is:

$$G_a(V_{mc}) = \sum_{i=0}^{M} N_a^i P_o^i(V_{mc}) g^i(V_{mc}) \tag{1}$$

where M is the number of distinct channel types in the apical membrane, and N_a^i, $P_o^i(V_{mc})$, and $g^i(V_{mc})$ are the surface density, the steady-state open probability, and the unitary conductance of channel type i, respectively. We take G_a to arise from only two channel types (see Results): background, voltage-independent, ohmic channels which can be lumped (G_a^0), and voltage-activated maxi K^+ channels. Then, Eq. 1 becomes:

$$G_a(V_{mc}) = G_a^0 + N_a P_o(V_{mc}) g(V_{mc}) \tag{2}$$

where $g(V_{mc})$, $P_o(V_{mc})$, and N_a now refer specifically to maxi K^+ channels. For data analysis, it is convenient to scale Eq. 2 by the basolateral membrane conductance (G_b), which is taken to be voltage independent, so that:

$$\frac{G_a(V_{mc})}{G_b} = \frac{G_a^0}{G_b} + \frac{N_a}{G_b} P_o(V_{mc}) g(V_{mc}) \tag{3}$$

$G_a(V_{mc})$ and $g(V_{mc})$ are measured experimentally, while G_a^0, N_a, and $P_o(V_{mc})$ are evaluated using Eqs. 2 and 3, as described below. The voltage dependence of G_a is ascribed solely to maxi K^+ channels on the basis of single-channel studies which indicated that these are the predominant voltage-activated K^+ channels in the apical membrane (see Results).

Measuring $g(V_{mc})$

The current-voltage (I–V) relation for maxi K^+ channels exposed to physiological K^+ and Na^+ concentrations was described using a simplified barrier rate model consistent with emerging views of multi-ion conduction in maxi K^+ channels (see Neyton and Miller, 1988). The channel is modeled as a pore containing five barriers of equal width and four wells of equal depth. The channel has a high affinity for K^+, and resides solely in high-occupancy states. Transitions among occupancy states obey microscopic reversibility. Energy barriers to K^+ movements within the pore are neglected. This model gives rise to an explicit expression for single-channel current containing three adjustable barrier rate constants. Single-channel slope conductance $g(V_m)$ is given by the derivative of this expression with respect to voltage.

Ca^{2+} and Voltage Dependencies of Channel Gating

Expressions relating single-channel open probability to V_m and $[Ca^{2+}]_i$ are developed empirically. For $[Ca^{2+}]_i$ equal to 0.1, 0.3, and 1 μM, the relationship between P_o and V_m is approximated by a Boltzmann relation:

$$P_o = \frac{P_o^{max}}{1 + e^{[-n_z F(V - V^0)/RT]}} \tag{4}$$

where P_o^{max} is maximum P_o, n_z describes the voltage sensitivity of the gating reaction, and V^0 is the membrane voltage at which P_o is half-maximal. The experimental results suggest that changing $[Ca^{2+}]_i$ in the range 0.1–1 μM shifts $P_o(V_m)$ along the voltage axis, without changing the voltage dependence of the gating reaction (see also Latorre et al., 1982; Methfessel and Boheim, 1982; Singer and Walsh, 1987; Reinhart et al., 1989). This observation allows P_o (V_m) data to be fitted simultaneously, assigning one value of V^0 to data obtained at a given $[Ca^{2+}]_i$, and one value of n_z to the combined data. Shifts of V^0 are roughly constant for half-log unit changes in $[Ca^{2+}]_i$, so that V^0 can be approximated by:

$$V^0 = a \log_{10}[Ca^{2+}]_i + b \tag{5}$$

where a and b are constants. Eq. 5 is used to estimate $[Ca^{2+}]_i$ in the intact gallbladder, where $[Ca^{2+}]_i$ is unknown, but V^0 can be estimated.

Measuring $G_a(V_{mc})$

Estimates of G_a and G_b at the resting apical membrane voltage are obtained from cable analysis experiments. $G_a(V_{mc})$ is determined over a range of V_{mc} values using 1-s transepithelial current clamps, as described in Materials and Methods. Calculations of G_a account for changes in G_a and E_a elicited by transepithelial current clamps (see Appendix).

Reconstructing $P_o(V_{mc})$ for Apical Membrane Channels

A three-step fitting procedure is used to estimate $P_o(V_{mc})$ for apical membrane maxi K^+ channels, as well as G_a^0 and N_a. In step 1, $G_a(V_{mc})/G_b$ data are used without correction for voltage-induced changes in G_a and E_a. These data are fitted to Eq. 3 with $P_o(V_{mc})$ described by a Boltzmann relation. Estimates are obtained for G_a^0/G_b,

N_a/G_b, n_z, and V^0. In step 2, best-fit parameters obtained in step 1 are substituted into Eq. 3 to generate a $G_a(V_{mc})/G_b$ curve that is representative of the pooled experimental points. Points on this curve are corrected for voltage-induced changes in G_a and E_a, as outlined in the Appendix. In step 3, the corrected points are fitted as in step 1, yielding revised estimates for G_a^0, N_a, n_z, and V^0. The revised estimates for n_z and V^0 define $P_o(V_{mc})$ for apical membrane channels according to Eq. 4.

RESULTS

Patch-Clamp Experiments

Maxi K^+ channels were identified in the apical membrane of the intact epithelium, and in dissociated epithelial cells. The low yield of patch-clamp studies on intact tissues precluded their use in detailed characterizations of apical maxi K^+ channels. Thus, the majority of our studies were carried out using dissociated cells, which were easily patched, and which exhibited maxi K^+ channels similar to those in the intact apical membrane, as demonstrated below.

Maxi K^+ channels in the apical membrane of the intact epithelium. Records from a cell-attached patch in the apical membrane of the intact epithelium are illustrated in Fig. 1. In this patch, obtained with the tissue bathed in NaCl Ringer's and with 100 mM KCl in the pipette solution, a single major channel type is evident, which activates when the membrane is depolarized. Single-channel current amplitude approaches zero as the membrane is depolarized, suggesting that the channels are primarily K^+ selective, inasmuch as the expected reversal potentials for K^+, Na^+, and Cl^-, estimated from previously determined membrane voltages and intracellular ionic activities (see Reuss, 1989), occur at $V_p = -60$ mV, $V_p \gg 0$ mV, and $V_p = -25$ mV, respectively.

Channel activity in a second patch excised from the apical membrane of the intact epithelium are shown in Fig. 2. Again, channel activity in the cell-attached configuration was low (Fig. 2 *A*). Excising the patch into a bathing solution containing 1 mM Ca^{2+} activated three channels of similar conductance. *I-V* relations for these channels are shown in Fig. 2 *C*. In symmetrical KCl solutions, the single-channel *I-V* relationship was linear, with a slope conductance of 162 pS, and a reversal potential of 3 mV. Reducing K^+ in the bath to 5 mM shifted the reversal potential to $V_m = 62$ mV, as expected for a K^+-selective channel. Assuming that the channels are permeable to Na^+ and K^+ only, application of the Goldman-Hodgkin-Katz equation yields an estimated K^+:Na^+ permeability ratio of 23:1.

The effects of applying 1 mM Ba^{2+} to the internal face of a patch exposed to symmetrical KCl solutions and 1 mM internal Ca^{2+} are illustrated in Fig. 3. In the absence of Ba^{2+}, single-channel open probability (P_o) was high and decreased slightly with depolarization; the latter effect may have been caused by a voltage-dependent low-affinity block by internal Ca^{2+} (Vergara and Latorre, 1983). Internal Ba^{2+} reduced single-channel P_o in a voltage-dependent manner, with more pronounced inhibition at positive membrane voltages.

These and other experiments on intact gallbladders ($n = 5$) indicate that the predominant channel in the apical membrane is a large conductance K^+ channel, which is activated by membrane depolarization. Because of their large conductance, Ca^{2+}

sensitivity, and voltage-dependent Ba^{2+} sensitivity, these channels classify among the maxi K^+ channels first described in nerve and muscle preparations, and later reported to be present in numerous epithelial systems.

Maxi K^+ channels in dissociated cells. Currents through a single maxi K^+ channel

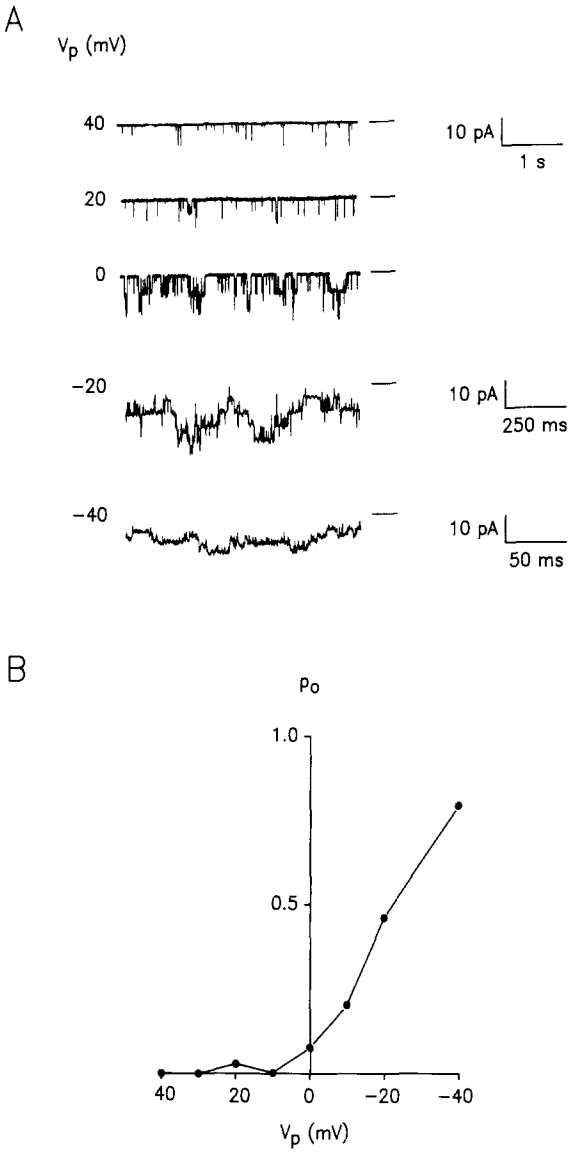

FIGURE 1. Single maxi K^+ channels in the apical membrane of the intact epithelium. (*A*) Recordings from a cell-attached patch in the apical membrane of the intact epithelium. The tissue was bathed in NaCl Ringer's; the patch relative to the bath. Downward deflections correspond to channel openings; baselines are indicated to the right of the current records. (*B*) Open probability P_o vs. V_p.

excised from a dissociated cell are shown in Fig. 4. In symmetrical KCl solutions, the *I-V* relation was linear, with a slope conductance of 199 pS, and a reversal potential of 0 mV. With 2.5 mM K^+ in the bath, the *I-V* relation rectified, and did not reverse in the membrane voltage range spanning −40 to 40 mV, placing a lower limit of 6:1

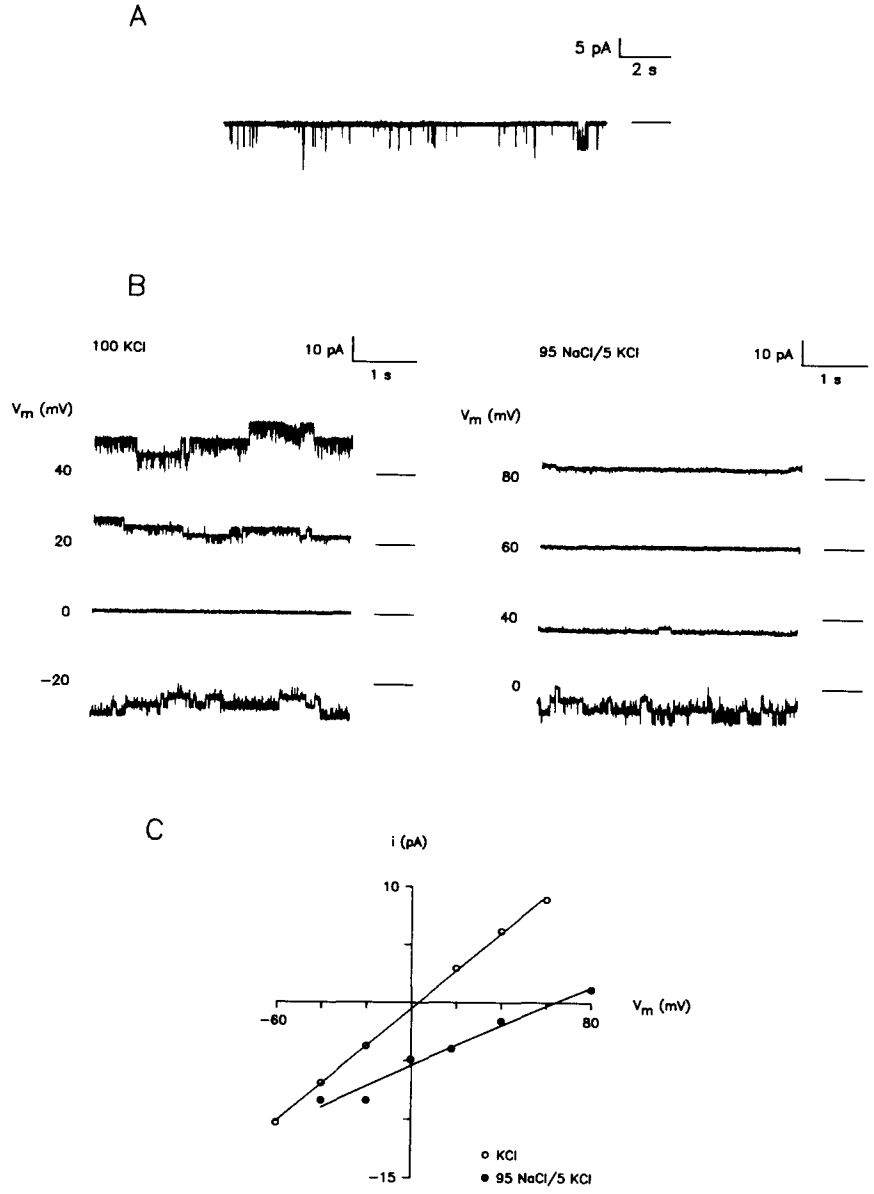

FIGURE 2. Ion selectivity and Ca^{2+}-dependent activation of apical membrane channels. (*A*) Channel activity in the cell-attached mode. The tissue was bathed in NaCl Ringer's; the patch pipette contained 100 mM KCl solution. V_p was held at 0 mV. (*B*) Channel activity in the inside-out configuration, with 100 mM KCl or 95 mM NaCl/5 mM KCl in the bath. Bath $[Ca^{2+}]$ was 1 mM. (*C*) Single-channel *I-V* relations in symmetrical KCl, or under Na^+:K^+ biionic conditions. Channels were activated by excision into a bathing solution containing 1 mM Ca^{2+}. Reducing internal K^+ from 100 to 5 mM shifted the channel reversal potential from 3 to 62 mV, as expected for a K^+-selective channel.

on the K^+:Na^+ permeability ratio. Replacing KCl in the bath with K gluconate had no effect on the *I-V* relation, confirming the anion impermeability of this channel. The single-channel conductance in symmetrical 100 mM KCl solution was 202 ± 12 pS (n = 7).

The effects of 1 mM internal Ba^{2+} on a maximally activated K^+ channel from a dissociated cell are summarized in Fig. 5. In the absence of Ba^{2+}, single-channel P_o was near 1 at all membrane voltages; there was no evidence of a decrease in P_o at positive membrane voltages. Internal Ba^{2+} reduced channel open probability in a voltage-dependent manner, with half-maximal inhibition at V_m = −19 mV, compared with V_m = −40 mV for maxi K^+ channels excised from the apical membrane of the intact tissue.

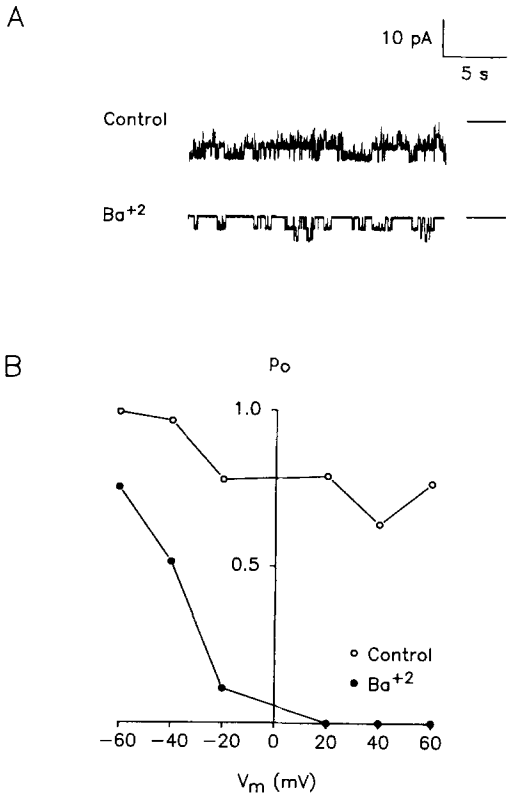

FIGURE 3. Ba^{2+} blockage of maxi K^+ channels from the apical membrane of the intact epithelium. (*A*) Channel activity in an inside-out patch is shown before and after addition of 1 mM Ba^{2+} to the bath. Records were obtained in symmetrical 100 mM KCl solutions, with $[Ca^{2+}]_i$ = 1 mM, and V_m = −20 mV. (*B*) Single-channel P_o measured as a function of membrane voltage. High P_o values determined in the absence of Ba^{2+} are due to the high $[Ca^{2+}]_i$. The effects of Ba^{2+} are voltage dependent, becoming clearest at $V_m > 0$, where no channel openings are observed.

The ion selectivity, unitary conductance, and Ba^{2+} sensitivity of maxi K^+ channels in the apical membrane of the intact epithelium and in dissociated cells suggest that these channels are similar, and validate the use of dissociated cells in studies in apical channels. Additional evidence for the apical membrane origin of maxi K^+ channels in dissociated cells rests on similarities between their Ca^{2+} and voltage sensitivities, examined below, and those of macroscopic G_a. Patterns of sensitivity to K^+ channel blockers provide another important basis for correlating maxi K^+ channels

and $G_a(V_{mc})$. Indeed, maxi K^+ channels and $G_a(V_{mc})$ exhibit similar patterns of sensitivity to Ba^{2+}, TEA^+, and quinine, and we will address this issue in a later report.

Single-channel I-V relations at physiologic K^+ and Na^+ concentrations. As a first step in relating single-channel and microelectrode data, *I-V* relations were collected for maxi K^+ channels exposed to solutions containing monovalent cations at physiologic concentrations (Fig. 6 *A*). The average *I-V* relation ($n = 3$) is shown in Fig. 6 *B*.

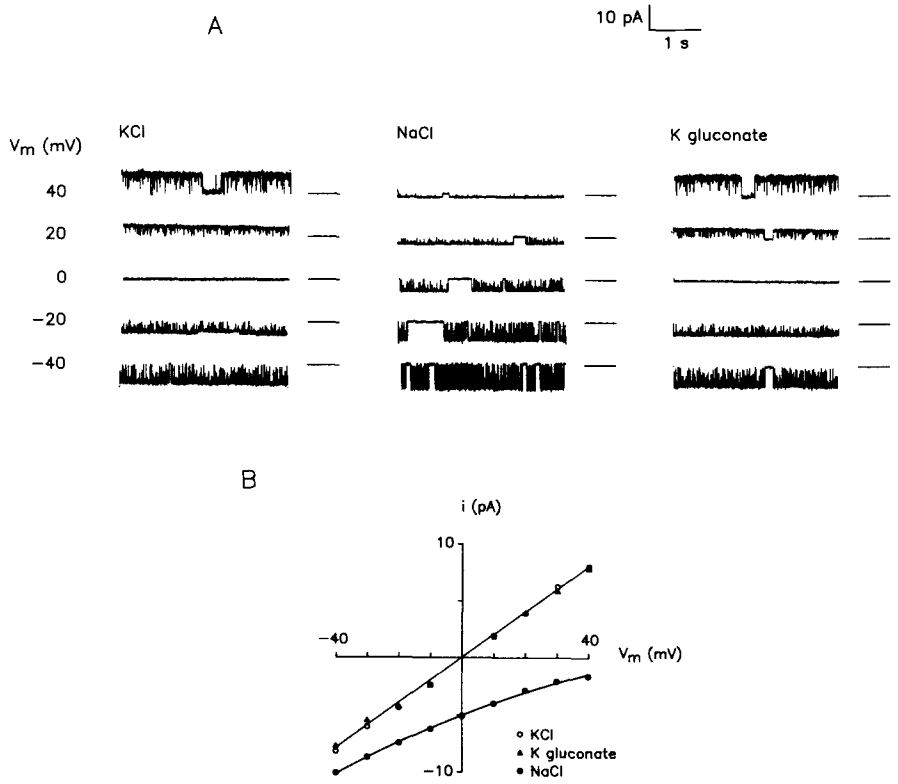

FIGURE 4. Ion selectivity of maxi K^+ channels from dissociated cells. *I-V* relations were obtained for a maxi K^+ channel in an inside-out patch. The patch pipette contained 100 mM KCl solution. (*A*) Channel activity observed with 100 mM KCl, 97.5 mM NaCl/2.5 mM KCl, or 100 mM K gluconate in the bath. Baselines are indicated to the right of the current records. (*B*) *I-V* relations determined under these three sets of ionic conditions. Reducing the internal $[K^+]$ from 100 to 2.5 mM shifted the reversal potential from 0 to >60 mV, while replacing KCl with K gluconate had no effect on the *I-V* relation.

As expected, the curve rectifies; current reversal is not observed in the experimental V_m range. In some systems, currents through maxi K^+ channels bathed in physiological gradients diminish as the membrane voltage is depolarized, reflecting internal Na^+ block (Marty, 1983). We did not observe diminution of the currents for $V_m <$ 30 mV.

Overlying the *I-V* relation in Fig. 6 *B* is the fitted curve given by a simple barrier

model of the channel pore (Fig. 6 *C*). Single-channel slope conductance $g(V_m)$, calculated as the derivative of the fitted *I-V* relation, is shown in Fig. 6 *D*.

Ca^{2+} and voltage dependencies of channel gating. Studies assessing the Ca^{2+} and voltage-dependencies of maxi K^+ channel steady-state P_o were carried out using inside-out patches from dissociated cells (Fig. 7). Channels were activated by membrane depolarization and by elevation of internal Ca^{2+} concentration. Channels exhibited wide quantitative variability in their Ca^{2+} and voltage sensitivities, as reflected by the large SEMs in Fig. 7. Variability in the Ca^{2+} and voltage sensitivities of maxi K^+ channels within experimental preparations has been noted previously

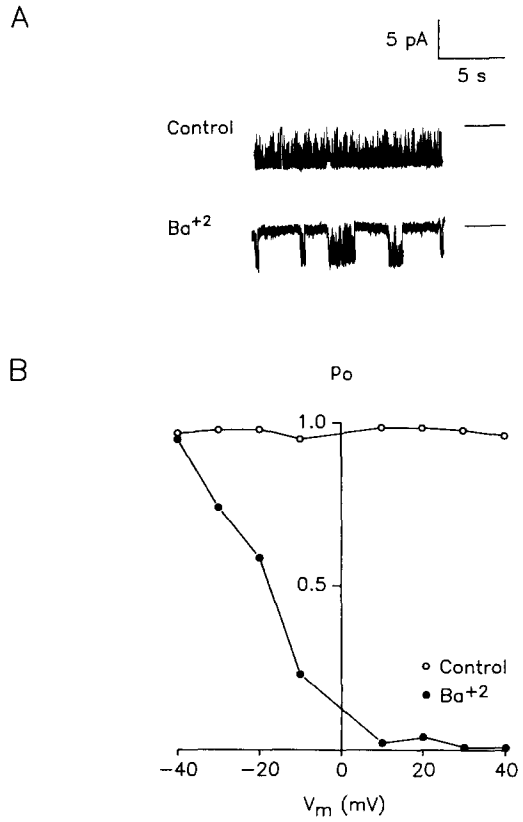

FIGURE 5. Ba^{2+} sensitivity of maxi K^+ channels from dissociated cells. An inside-out patch was bathed symmetrically in 100 mM KCl, with $[Ca^{2+}]_i$ = 1 mM, sufficient for maximal activation of the channels. Ba^{2+} was added to the bath to a final concentration of 1 mM. (*A*) Channel activity at −20 mV, before and after addition of 1 mM Ba^{2+}. (*B*) Single-channel P_o as a function of V_m, before and after Ba^{2+} addition. Ba^{2+} block was voltage dependent, increasing *e*-fold/15 mV in the range of −40 to 10 mV. Half-maximal block occurred at −19 mV, compared with −40 mV for maxi K^+ channels from the intact apical membrane.

(Moczydlowski and Latorre, 1983; Singer and Walsh, 1987). At V_m = 0 mV, single-channel P_o was half-maximal at roughly 400 nM Ca^{2+}, which is low in comparison to the half-maximal activation concentrations reported for excitable cells (Latorre, 1986; Blatz and Magleby, 1987) and some epithelia (Christensen and Zeuthen, 1987; Merot et al., 1989), typically 1–10 μM, but similar to those for channels in other epithelia (Kolb et al., 1986; Maruyama et al., 1986; Sheppard et al., 1988).

The best-fit parameters obtained when P_o vs. V_m curves in Fig. 7 were fitted individually to Boltzmann expressions are summarized in Table I (fit I). As expected,

elevating internal Ca^{2+} shifted V^0 in the negative direction. Further, as internal Ca^{2+} was increased, n_z decreased, suggesting that the channel-gating mechanism becomes less voltage dependent at higher $[Ca^{2+}]_i$. We tested the alternative possibility that the voltage dependence of the gating reaction is in fact independent of $[Ca^{2+}]_i$, as

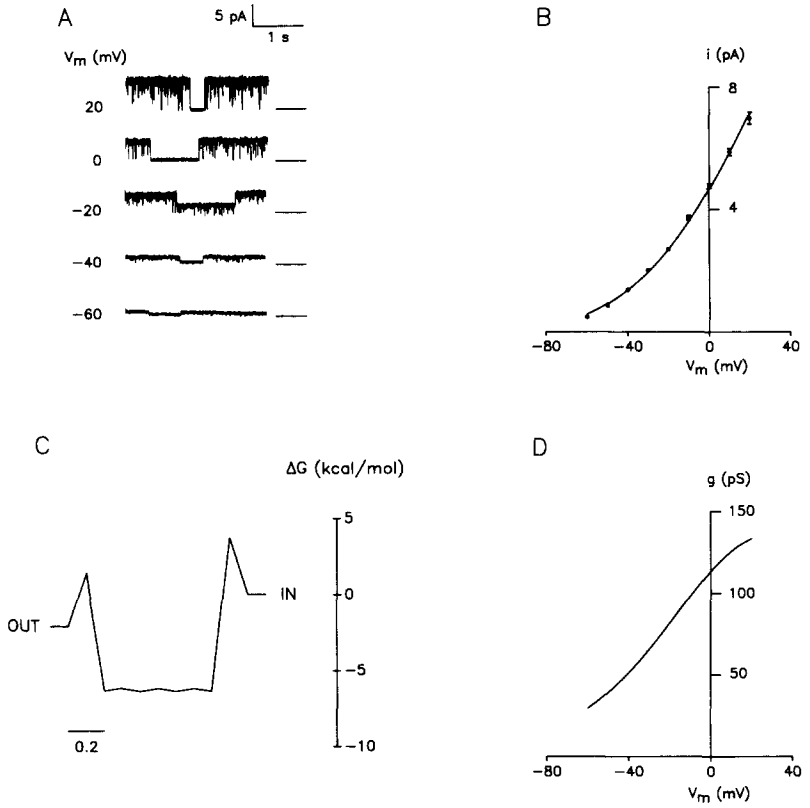

FIGURE 6. Conduction across maxi K^+ channels exposed to physiologic Na^+ and K^+gradients. Inside-out patches were bathed in solutions containing physiological concentrations of monovalent cations (see Materials and Methods for solution compositions). (*A*) Channel activity. Baselines appear to the right of the current records. (*B*) Average *I-V* relation ($n = 3$). The solid line depicts the best fit to the simple barrier model. (*C*) Barrier model for K^+ permeation, described in Models. The model is shown for the case of 0 mV applied voltage; the difference in the internal and external solution free energy levels reflects the K^+ concentration gradient across the membrane. (*D*) Single-channel slope conductance $g(V_m)$, given by the derivative of the fitted *I-V* relation with respect to voltage.

first proposed by Latorre et al. (1982). The P_o data shown in Fig. 7 were fitted simultaneously to the Boltzmann equation, assigning one value of n_z to the combined sets of points, and one value of V^0 for each set of points (fit II). The curves resulting from this fit overlie the data in Fig. 7. V^0 was linearly dependent on

$\log_{10}[Ca^{2+}]_i$ (see Eq. 5), according to

$$V^0 = -94 \log_{10}[Ca^{2+}]_i - 36 \tag{6}$$

with $[Ca^{2+}]_i$ given in micromolar.

If Eq. 5 holds, then the Boltzmann relation can be rewritten in the form:

$$P_o = \frac{P_o^{max}}{1 + K[Ca^{2+}]_i^{-N} e^{(-n_z FV/RT)}} \tag{7}$$

where $K = \exp(bn_zF/RT)$, and $N = an_zF/2.303\ RT$. Precise reaction schemes that

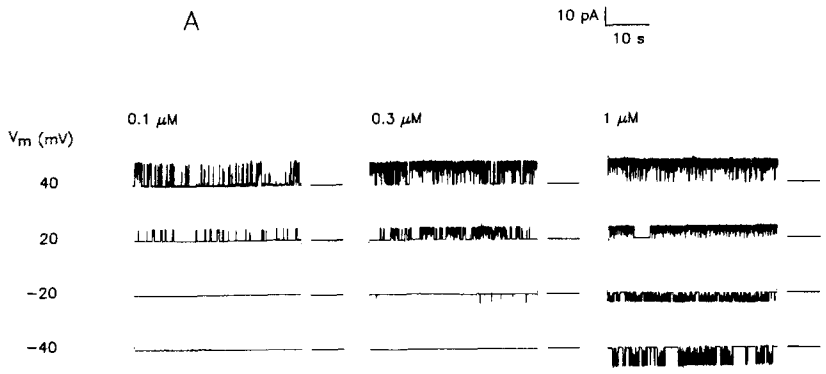

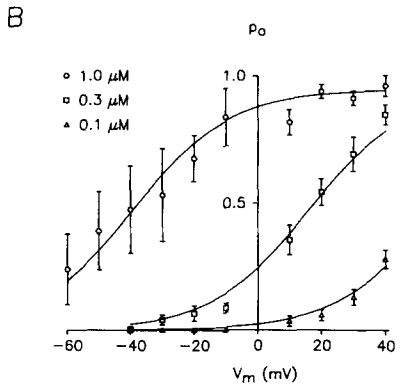

FIGURE 7. Ca^{2+} and voltage dependence of maxi K^+ channel P_o. Inside-out patches from dissociated cells were exposed symmetrically to 100 mM KCl, with internal Ca^{2+} buffered to 0.1, 0.3, or 1 μM. (*A*) Maxi K^+ channel in a single inside-out patch is shown over ranges of $[Ca^{2+}]_i$ and membrane voltage. (*B*) Ca^{2+} and voltage dependence of P_o, summarized from five experiments; each point represents the mean value determined from at least four of the experiments. Curves overlying the data represent the results of fits to Boltzmann relations (see Table I and text for details), with $n = 1.6$ for the three sets of data, and $V^0 = 56$, 16, and -39 for 0.1, 0.3, and 1 μM Ca^{2+}, respectively. P_o, single-channel open probability; n, number of gating charges; V^0, membrane voltage at which P_o is half-maximal.

can give rise to an expression of this form have been described previously (Methfessel and Boheim, 1982). In an attempt to incorporate the effects of internal Ca^{2+} and V_m into a single expression for P_o, data in Fig. 7 were fitted simultaneously to Eq. 7, with the results shown in Table I (fit III). This model predicted a shallower voltage dependence for P_o than did fit II; curves resulting from this fit (not shown) failed to describe the steep regions of $P_o(V_m)$ for $[Ca^{2+}]_i$ equal to 0.1 and 0.3 μM. It is possible that Eq. 7 can in fact represent the data, and that use of V^0 in fit II "loosens" the equation, allowing for small deviations in the specified values of $[Ca^{2+}]_i$. Regardless, for the purpose of relating single-channel data to microelectrode data, we settled on the results of fit II, which provide a reasonable description of the data with a minimum number of adjustable parameters.

Time scale of channel activation. The single-channel functions $P_o(V_{mc})$ and $g(V_{mc})$ represent the steady-state determinations. To relate these functions to the macro-

TABLE I

Single-Channel Open Probability Described Using Boltzmann Relations

Fit	$[Ca^{2+}]_i$	P_o^{max}	n	V^0
	μM			mV
I	0.1	0.96	2.2	50
	0.3	0.96	2.0	17
	1	0.96	1.4	−37
II	0.1	0.95	1.6	56
	0.3	0.95	1.6	16
	1	0.95	1.6	−39
	P_o^{max}	n	K	N
III	0.96	1.5	0.11	2.6

Single-channel P_o was measured as a function of V_m, at 0.1, 0.3, and 1 μM Ca^{2+} (see text and Fig. 10). Values represent best-fit Boltzmann parameters. Fit I: sets of $P_o(V_m)$ data were fitted individually to the Boltzmann equation. Fit II: sets of $P_o(V_m)$ data were fitted simultaneously to Boltzmann relations, assigning one value of V^0 to each set of data, and one value of n to the combined sets of data. Fit III: data were fitted simultaneously to Eq. 8 (see text). P_o^{max}, maximum P_o; n, number of gating charges; V^0, membrane voltage at which $P_o = P_o^{max}/2$; K, effective voltage- and Ca^{2+}-dependent equilibrium constant; N, Ca^{2+} Hill coefficient.

scopic G_a, it is necessary to establish that microelectrode experiments also assess steady-state channel activity. Changes in apical membrane conductance elicited by transepithelial current clamps reach stable values within 200 ms (Stoddard and Reuss, 1988*b*), suggesting that channel activation is complete within this time frame. To further verify that gallbladder maxi K^+ channels reach steady-state gating within 800 ms, voltage-step experiments were carried out using inside-out patches exposed to symmetrical 100 mM KCl and 500 nM internal Ca^{2+}. In the experiment summarized in Fig. 8, stepping V_m from −40 to 20 or 40 mV activated up to five channels in the patch. The ensemble currents assembled from the individual steps reveal that for steps to 20 mV, the shift from $P_o = 0$ to the new steady-state P_o of 0.30 is essentially complete at 800 ms. The same is true for steps to 40 mV, where P_o increases to 0.65. The rapid establishment of gating steady state validates the use of 800-ms time

points in comparisons between microelectrode measurements and steady-state single-channel data. Steps from −40 mV to V_m in the range of 10 to 40 mV did not reveal secondary channel inactivation processes, which have been observed with maxi K^+ channels from cultured rat muscle (Pallotta, 1985).

Microelectrode Experiments

Previous studies in this and other laboratories have revealed that the cable properties of *Necturus* gallbladder epithelium depend on the composition of bathing Ring-

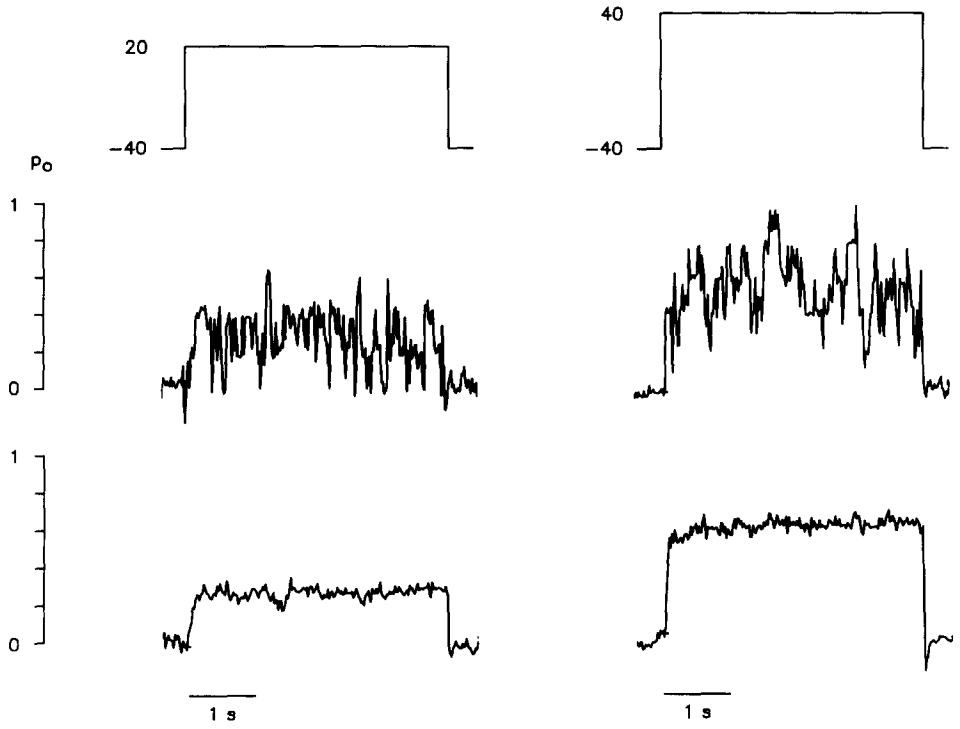

FIGURE 8. Time course of maxi K^+ channel activation. Channels in an inside-out patch exposed symmetrically to 100 mM KCl, with $[Ca^{2+}]_i$ = 500 nM, were subjected to depolarizing steps from −40 mV to 20 or 40 mV. Depolarizing steps caused activation of up to five channels. (*Top traces*) Holding voltage. (*Middle traces*) Channel activity elicited by single voltage steps to 20 or 40 mV. (*Bottom traces*) Ensemble currents assembled from multiple steps (n = 50 for steps to 20 mV; n = 30 for steps to 40 mV). P_o, single-channel open probability. The ensemble currents indicate that channel activation is essentially complete within 800 ms after the voltage step.

er's solution and on the measurement techniques (see Stoddard and Reuss, 1988*a*). To allow comparisons between single-channel and microelectrode data, we measured the cable properties of four tissues bathed in 10 mM HEPES-buffered Ringer's. The results of these experiments are summarized in Table II. The apical and basolateral membrane conductances were 180 and 350 $\mu S/cm^2$, respectively.

To assess the voltage dependence of the macroscopic apical membrane conductance, we carried out a series of current-clamp experiments, summarized in Fig. 9 *A*.

TABLE II

Equivalent Circuit Parameters for Gallbladders Bathed in 10 mM HEPES Ringer's

Resistances				
R_a/R_b	R_t	R_a	R_b	R_s
	Ω-cm^2	Ω-cm^2	Ω-cm^2	Ω-cm^2
2.0 ± 0.4	105 ± 18	5,500	2,800	106

Voltages and EMFs				
V_{mx}	V_{mc}	V_{cs}	E_a	E_b
		mV		
0 ± 1	−68 ± 2	−68 ± 2	−68	−68

Values are mean ± SEM of four experiments. Values without SEM were determined from the steady-state equivalent circuit model (see Reuss and Finn, 1975*a*). R_a, apical membrane resistance; R_b, basolateral membrane resistance; R_t, transepithelial resistance; R_s, paracellular resistance; V_{mx}, transepithelial voltage; V_{mc}, apical membrane voltage; V_{cs}, basolateral membrane voltage; E_a, apical membrane equivalent EMF; E_b, basolateral membrane equivalent EMF. $\Delta V_{cs}(x)$ was measured as described in Materials and Methods. The pooled experimental points were fitted to a zero-order Bessel function (see Reuss and Finn, 1975*a* for details), yielding a space constant λ of 297 μm, and an A_0 value of 16.9 mV; these values for λ and A_0 lead to an estimate of 1,900 Ω-cm^2 for R_z (the resistance of R_a and R_b in parallel).

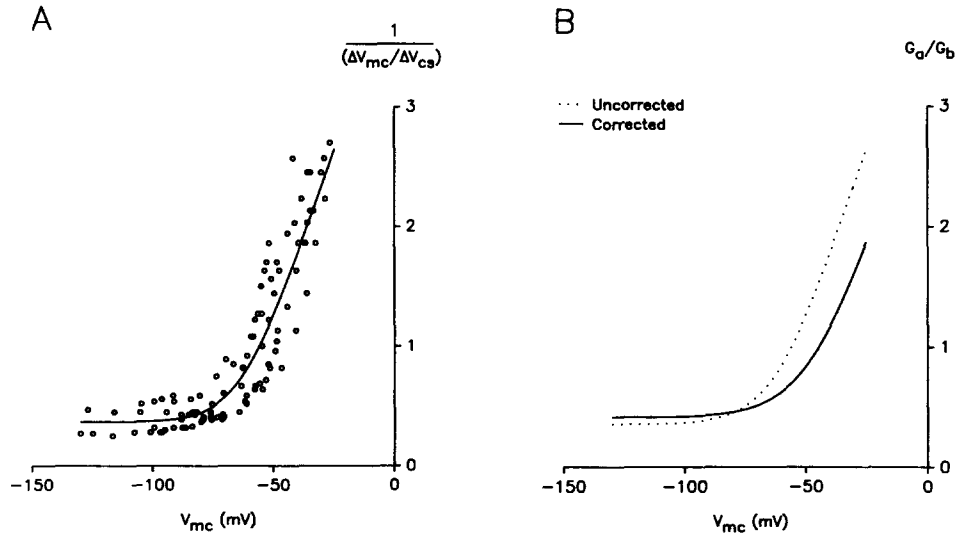

FIGURE 9. Voltage dependence of G_a/G_b. (*A*) $1/(\Delta V_{mc}/\Delta V_{cs})$ vs. V_{mc} data were pooled for six current-clamp experiments. The solid line represents the best fit to Eq. 3 (see Table II). (*B*) G_a/G_b corrected for voltage-induced changes in G_a and E_a. (*Dotted line*) Fitted curve describing uncorrected G_a/G_b curve, transposed from *A*. (*Solid line*) Fitted curve describing corrected G_a/G_b curve, with $G_a^0/G_b = 0.43$, $N_a^0/G_b = 2.5 \times 10^{-4}$ $\mu m^{-2}/(\mu S/cm^2)$, $n = 1.6$ and $V^0 = -46$ mV.

It is evident that as V_{mc} is depolarized, the apparent ratio of cell membrane conductances rises considerably, as previously observed (García-Díaz et al., 1983; Stoddard and Reuss, 1988*b*). The increase in apparent G_a/G_b is due to changes in G_a, i.e., to activation of conductive pathways in the apical membrane (García-Díaz et al., 1983; Stoddard and Reuss, 1988*b*). In light of the present work, maxi K^+ channels are likely to account for this increase in conductance.

Correlation of Single-Channel and Microelectrode Data

Single maxi K^+ channels and macroscopic G_a are related by Eqs. 2 and 3. In the first step of the three-step process for fitting $G_a(V_{mc})/G_b$ (see Models), uncorrected G_a/G_b data were fitted to Eq. 3, with $P_o(V_{mc})$ given by a Boltzmann relation. The resulting best-fit parameters are shown in Table III; the best-fit curve is shown in Fig. 9 *A*. This curve provides a reasonable description of the pooled data, but deviates from

TABLE III

Reconstruction of the Apical Membrane Conductance $G_a(V_{mc})$

	G_a^0/G_b	G_a^0	N_a/G_b	N_a	n	V^0
	Uncorrected G_a/G_b data					
		$\mu S/cm^2$	$\mu m^{-2}/(\mu S/cm^2)$	$1/\mu m^2$		mV
	0.37	130	3.4×10^{-4}	0.12	2.1	−60
	Corrected G_a/G_b data					
Fixed n	0.42	150	2.6×10^{-4}	0.09	1.6	−45
Varying n	0.43	150	2.5×10^{-4}	0.09	1.8	−46

Values represent best-fit parameters obtained from fitting G_a/G_b data to Eq. 3. Uncorrected data were estimated from $1/(\Delta V_{mc}/\Delta V_{cs})$, as described in Materials and Methods. Corrected G_a/G_b data were obtained as described in the Appendix. Fixed n: n is fixed at 1.6, the value determined in single-channel studies. Varying n: n is adjustable. G_a, apical membrane conductance; G_b, basolateral membrane conductance; G_a^0, baseline apical membrane conductance; N_a, apical membrane maxi K^+ channel surface density; n and V^0 are defined in the legend to Table I. Estimates for G_a^0 and N_a were obtained by multiplying G_a^0/G_b and N_a/G_b by 350 $\mu S/cm^2$, the value of G_b determined in cable analysis experiments.

the true $G_a(V_{mc})/G_b$ relation, inasmuch as estimation of G_a/G_b from $1/(\Delta V_{mc}/\Delta V_{cs})$ neglects the voltage dependence of G_a and E_a (see Appendix). In the second step at the fitting process, the G_a/G_b relation was corrected for voltage-induced changes in G_a and E_a. As shown in Fig. 9 *B*, uncorrected G_a/G_b values deviate from corrected G_a/G_b values as the magnitude of ΔV_{mc} increases, underestimating G_a/G_b by 9% at $V_{mc} = -100$ mV, and overestimating G_a/G_b by 43% at $V_{mc} = -25$ mV.

Although the region of overlap between single-channel and microelectrode data is restricted to the voltage range of −25 to −60 mV, we chose, in the third step of the fitting procedure, to fit the entire range of $G_a(V_{mc})$, with the results shown in Table III. When the fit was confined to the region of overlap, the best-fit parameters differed by less than 10% from those showed in Table III.

The results of the fit indicate that the leakage conductance of G_a^0 is roughly 150 $\mu S/cm^2$, or 83% of the control apical membrane conductance of 180 $\mu s/cm^2$. The

remaining portion of control G_a can be accounted for by maxi K^+ channels, which are present at a surface density of $0.09/\mu m^2$, and which have a P_o of 0.15 and a slope conductance of ~23 pS at control V_{mc}. Depolarizing V_{mc} increases macroscopic G_a as a result of both channel rectification and channel activation, inasmuch as channels at resting V_{mc} operate at the foot of the activation curve (see Fig. 10). The membrane voltage at which P_o is half-maximal (V^0) is −45 mV. If the Ca^{2+} and voltage dependencies of channel gating are assumed to be similar in situ and in excised patches, as appears to be the case in other cells (Pallotta et al., 1987), then Eq. 6 yields an estimate of 1.2 μM for free [Ca^{2+}] near the channel regulatory site. That is, channel activity is higher than predicted from the bulk cytosolic Ca^{2+} activity of 100–200 nM, measured using intracellular microelectrode techniques (Palant and Kurtz, 1986). Possible mechanisms accounting for the apparent enhancement of apical membrane maxi K^+ channel activity are considered in the Discussion.

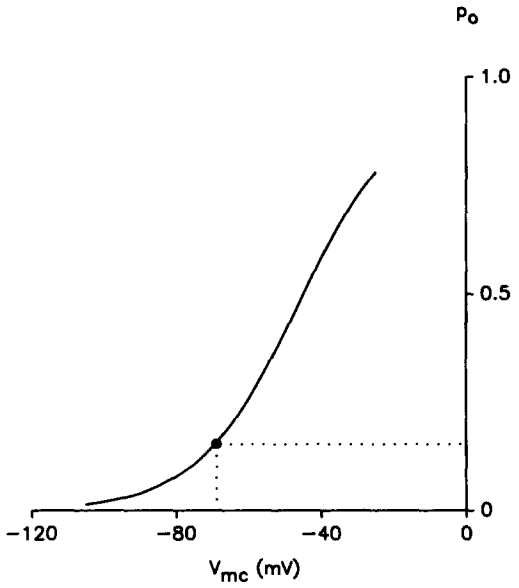

FIGURE 10. Reconstructed $P_o(V_{mc})$ curve for apical membrane maxi K^+ channels. The curve is given by a Boltzmann relation (Eq. 4), with $P_o^{max} = 0.94$, $n_z = 1.9$ and $V^0 = -46$ mV. Dotted lines denote control V_{mc} and P_o values of −68 mV and 0.12, respectively. This is the shape that $P_o(V_{mc})$ must take to account for the voltage dependence of the apical membrane conductance.

DISCUSSION

Maxi K^+ Channels in Gallbladder Epithelium

The apical membrane of *Necturus* gallbladder epithelium is predominantly K^+ conductive, and displays a small Na^+ conductance (Reuss and Finn, 1975*a*, *b*). Ordinarily, the apical membrane is the dominant resistance to transepithelial current flow, accounting for 60–90% of the transcellular resistance, although apical membrane resistance can be lowered by numerous factors, including membrane depolarization (García-Díaz et al., 1983; Stoddard and Reuss, 1988*b*), elevation of intracellular Ca^{2+} (Bello-Reuss et al., 1981; García-Díaz et al., 1983) or cAMP levels (Petersen and Reuss, 1983), and extracellular alkalinization (Reuss et al., 1981). The

apical membrane K^+ conductance in guinea pig gallbladder is also Ca^{2+} and voltage sensitive (Gunter-Smith, 1988).

In this paper, we describe single channels whose properties would explain the depolarization-induced, Ca^{2+}-activated apical membrane K^+ conductance in *Necturus* gallbladder. In cell-attached patches, these channels open infrequently at the resting apical membrane voltage, and activate with membrane depolarization. In excised, inside-out patches from the apical membrane of the intact epithelium, these channels are more than 20-fold selective for K^+ over Na^+, display a large unitary conductance (>150 pS) in symmetrical KCl solutions, and are blocked in a voltage-dependent manner by 1 mM internal Ba^{2+}. Similar large conductance K^+ channels are observed in patches excised from dissociated gallbladder cells. Like apical membrane K^+ channels, maxi K^+ channels from dissociated cells are more than 10-fold selective K^+ over Na^+ and are blocked in a voltage-dependent manner by internal Ba^{2+} ions. In addition, they are activated by membrane depolarization and by elevation of internal Ca^{2+} levels.

Origin of Gallbladder Maxi K^+ Channels

The ion selectivity, unitary conductance, and Ca^{2+} and Ba^{2+} sensitivities of maxi K^+ channels from dissociated cells suggest that these channels are similar to those in the intact apical membrane. Three additional items of evidence further support the notion that maxi K^+ channels are of apical membrane origin. First, the Ca^{2+} and voltage sensitivities of these channels parallel those of the macroscopic apical membrane conductance, i.e., both activate with membrane depolarization and elevation of intracellular Ca^{2+} levels. Second, these channels and the voltage-dependent component of the macroscopic conductance exhibit similar patterns of sensitivity to the K^+ channel blockers Ba^{2+} and TEA^+ (Segal and Reuss, in press). Third, recent studies on dissociated cells isolated from cAMP-stimulated gallbladders reveal small-conductance (10 pS) Cl^- channels which colocalize with maxi K^+ channels (Segal and Reuss, 1989). Since cAMP activates an apical membrane Cl^- conductance (Petersen and Reuss, 1983), it is likely that patches containing single Cl^- channels originate in the apical membrane. The notion that the apical membrane domain remains accessible in the plasma membrane of dissociated cells is supported by morphological studies on dissociated rat small intestinal epithelial cells (Ziomek et al., 1980; Bjorkman et al., 1986). In these systems, apical membrane markers such as microvilli or enzyme activities redistribute uniformly around the cell within minutes after dissociation.

Taken together, these pieces of evidence suggests that channels originating in the apical membrane remain accessible in dissociated cells. Although these arguments are indirect and do not strictly exclude the possibility that the channels under study are basolateral, the lack of voltage dependence of the basolateral membrane argues against the presence of maxi K^+ channels in this membrane (García-Díaz et al., 1983; Stoddard and Reuss, 1988*b*). Basolateral membrane maxi K^+ channels, considered hypothetically, do not have serious implications for our model, for the following reasons: first, the voltage and Ca^{2+} sensitivities of the channels are not expressed in situ (i.e., G_b is constant), and second, these channels, if studied in excised patches, are similar to apical membrane channels in the intact epithelium.

Definitive localization of maxi K^+ channels will require further patch-clamp studies on the intact epithelium, and morphological studies, which will be made possible when probes for maxi K^+ channels become available.

Apical membrane maxi K^+ channels in *Necturus* gallbladder are similar to those observed in numerous leaky NaCl-absorbing epithelia, including *Triturus* gallbladder (Maruyama et al., 1986), *Necturus* proximal tubule (Kawahara et al., 1987), and primary cultures of rabbit proximal tubule cells (Merot et al., 1989). Basolateral membrane K^+channels from leaky epithelia exhibit markedly different properties. The basolateral membrane of *Necturus* proximal tubule contains at least two types of K^+ channels, which have unitary conductances of <50 pS, and which are inactivated by membrane depolarization (Sackin and Palmer, 1987; Kawahara et al., 1987). The basolateral membrane of rabbit proximal tubule contains a K^+ channel that shows sharp inward rectification in symmetrical high K^+, and that is weakly activated by membrane depolarization (Parent et al., 1988). Basolateral maxi K^+ channels have been identified in studies on dissociated enterocytes from rat and *Necturus* small intestine (Morris et al., 1986; Sheppard et al., 1988). Consistent with this observation, the small intestine mounted in vitro responds to apical membrane depolarization with an increase in basolateral membrane K^+ conductance, rather than an increase in apical membrane K^+ conductance (Grasset et al., 1983).

Relating Single Maxi K^+ Channels to the Apical Membrane Conductance

The common properties shared by the voltage-dependent component of the macroscopic apical membrane K^+ conductance and single maxi K^+ channels suggest a link between the two. To account for the macroscopic conductance in quantitative terms, we have used simple models to describe steady-state conduction and gating properties of maxi K^+ channels. Our analysis is based on the assumption that conduction and gating are distinct processes that can be studied separately, each under optimal experimental conditions. For instance, in studies examining conduction at physiological Na^+ and K^+ concentrations, channels were activated with high Ca^{2+}, in order to obtain well-resolved transitions between open and closed states, and accurate estimates of the single-channel current amplitude. Analogously, in studies examining channel gating, patches were bathed in symmetrical K^+, rather than physiological K^+ and Na^+concentrations, to enhance the channel signal-to-noise ratio in the physiological V_m range.

Steady-state conduction through channels exposed to physiological $K^+$and Na^+ concentrations was described using a simplified barrier model, which borrows from multi-site models developed to describe conduction through maxi K^+ and other K^+ channels (Hodgkin and Keynes, 1955; Hille and Schwarz, 1978; Neyton and Miller, 1988). The Ca^{2+} and voltage dependencies of channel gating were analyzed empirically using Boltzmann relations. Kinetic analyses provide another means of describing $P_o(Ca^{2+}, V_{mc})$ (see Moczydlowski and Latorre, 1983), but such analyses are complex for maxi K^+ channels (McManus and Magleby, 1988), and beyond the scope of this paper. The expressions linking single-channel conductance and gating to macroscopic apical membrane conductance (Eqs. 2 and 3) give rise to estimates for the surface density and voltage-dependent P_o of apical membrane maxi K^+ channels.

Single-channel P_o at the resting apical membrane voltage is roughly 0.15, and increases steeply with membrane depolarization to a value of 0.78 at $V_{mc} = -25$ mV. A reexamination of two cell-attached patch experiments reveals the same pattern. Assuming that V_{mc} equals -70 mV in cell-attached patch experiments, the P_o values in one experiment, shown in Fig. 1, increased from 0.08 at $V_{mc} = -70$ mV to 0.79 at $V_{mc} = -30$ mV; in the second experiment (not shown), P_o increased from 0.01 to 0.84. In these experiments, P_o at resting V_{mc} was less than the value of 0.15 estimated from intracellular microelectrode experiments. Inasmuch as the number of cell-attached patch-clamp experiments is small, the significance of this difference is unclear. Regardless, the best-fit parameters describing $G_a(V_{mc})$ and results of cell-attached patch studies support the same conclusion, namely, that P_o is low at control V_{mc}, and that the steep increase in apical membrane conductance accompanying even small depolarizations (see Fig. 10) arises from both channel activation and outward rectification of the single-channel *I-V* relation. The $P_o(V_{mc})$ curves steepen at more negative membrane voltages than those predicted on the basis of inside-out patch studies (Fig. 7), if the intracellular free Ca^{2+} concentration is taken to be 100–200 nM (see Palant and Kurtz, 1986). Previous studies on rabbit cortical collecting tubule (Hunter et al., 1986) and *Necturus* choroid plexus (Christensen and Zeuthen, 1987) have noted that apical (or ventricular) membrane maxi K^+ channel activity is higher than predicted from bulk cytosolic Ca^{2+} levels.

Accounting for Apical Membrane Maxi K^+ Channel Activity

There are several possible explanations for the higher-than-expected activity of apical membrane maxi K^+ channels. First, the regulation of channels in excised patches may differ from regulation in situ, e.g., by loss of a channel-activating factor. Besides membrane voltage and intracellular Ca^{2+} levels, pH (Cook et al., 1984; Christensen and Zeuthen, 1987), and Mg^{2+}(Golowasch et al., 1986), and membrane surface charge (Moczydlowski et al., 1985) can regulate maxi K^+ channel activity. A second possibility is that maxi K^+ channel activity in situ is heightened by elevated Ca^{2+} levels in the immediate vicinity of the apical membrane. If the Ca^{2+}- and voltage-dependent mechanisms governing channel behavior in the intact epithelium and in cell-excised patches are similar, as has been demonstrated for maxi K^+ channels from other tissues (Pallotta et al., 1987), then it follows from our estimate of V^0 (-45 mV) that free Ca^{2+} levels near the channel regulatory sites are 1–2 μM. Steady-state elevations in internal Ca^{2+} near the apical membrane surface would require a constitutive Ca^{2+} influx, e.g., through Ca^{2+}-permeable channels, bile-acid anion-mediated pathways (Montrose et al., 1988), or sites of membrane damage, and means of rapidly buffering incoming Ca^{2+} ions. A final possibility is that maxi K^+ channels are not the only K^+ channels that underlie the voltage-dependent component of G_a. To play a role in the voltage activation of G_a, a second channel type would need to satisfy the following requirements: (*a*) marked outward rectification of the single-channel *I-V* relation, and/or activation with membrane depolarization; (*b*) susceptibility to block by external TEA^+ and Ba^{2+}; and (*c*) undetectability in patch-clamp experiments, by virtue of a small unitary conductance, low frequency of transitions between open and closed states, or tendency to run down in cell-excised patches.

Significance of G_a^0 and N_a

Two additional parameters emerge from reconstruction of $G_a(V_{mc})$, namely the leakage conductance G_a^0 and the apical membrane maxi K^+ channel surface density N_a. Given the estimate of 150 $\mu S/cm^2$ for G_a^0 and the total G_a of 180 $\mu S/cm^2$ at control V_{mc}, it follows that the effective equilibrium potential of channels underlying G_a^0 must be -64 mV, to account for the control apical membrane equivalent EMF of -68 mV. That is, the leakage conductance is predominantly K^+ selective, and probably harbors the small Na^+ permeability of the apical membrane (Reuss and Finn, 1975*a*, *b*). We have yet to identify the channels that underlie G_a^0. Difficulties in their identification would be expected if they have small unitary conductance and rarely close, like apical membrane K^+ channels recently described in rat renal cortical collecting tubule (Frindt and Palmer, 1989).

Estimates for the surface density of apical (or ventricular) membrane maxi K^+ channels are $0.06/\mu m^2$ in MDCK cells (Bolívar and Cereijido, 1987), $0.24/\mu m^2$ in *Triturus* gallbladder (Maruyama et al., 1986), and $0.4–0.9/\mu m^2$ in *Necturus* choroid plexus (Christensen and Zeuthen, 1987). Our estimate of 0.09 μm^2, appears to fall within this range, and slightly outside the range ($0.1–1.9/\mu m^2$) estimated for apical membrane K^+ channels in *Necturus* gallbladder on the basis of fluctuation analysis techniques (Gögelein and van Driessche, 1981). Importantly, our estimates are referred to μm^2 of stretched epithelium, rather than the true surface area of the apical membrane, which contains microvilli. It is also possible to estimate N_a based on the number of channels in membrane patches, and the patch surface area. Patches from the apical membrane of the intact epithelium contained 2.6 ± 0.7 channels/patch ($n = 5$). To match N_a determined from macroscopic G_a, patch areas corresponding to 30 μm^2 of stretched epithelium would be required. Total patch areas of 25 μm^2 are in the upper range of those determined for chromaffin cells and neuroblastoma (Sakmann and Neher, 1983); thus, it would appear than $0.1/\mu m^2$ is the lower limit on N_a estimated from the number of channels per path. Without capacitance measurements in our studies, the true surface area of patches excised from the folded apical membrane remains unknown.

Function of Maxi K^+ Channels in Gallbladder Equilibrium

The channels described here classify among the Ca^{2+}-activated maxi K^+ channels first observed in nerve and muscle preparations, and later identified in the apical membrane of numerous epithelia. In *Necturus* gallbladder, maxi K^+ channels are unlikely to contribute substantially to the baseline K^+ permeability of the apical membrane, though their expected contribution (17%) exceeds that estimated for maxi K^+ channels in other epithelia (Frindt and Palmer, 1987). In light of their steep voltage and Ca^{2+} sensitivities, it is more likely that maxi K^+ channels are important in cellular responses to physiological perturbations. These channels are equipped to repolarize the cell membrane voltage in response to agents which depolarize the apical membrane, and to promote KCl loss in response to cell swelling.

Maxi K^+ channels may also provide a pathway for transcellular K^+ secretion, which has been demonstrated in *Necturus* gallbladder (Reuss, 1981), and which is favored by the electrochemical gradient for K^+ movement across the apical mem-

brane. The sensitivities of the channels to membrane voltage and Ca^{2+} suggest that transcellular K^+ secretion may be a highly regulated process. This is probably of secondary importance in leaky NaCl-absorbing epithelia like the gallbladder, in which transcellular K^+ secretion is matched by paracellular absorption (Reuss, 1981), but may be crucial in K^+-secreting tight epithelia, like the mammalian cortical collecting tubule (see Hunter et al., 1984, 1986; Frindt and Palmer, 1987). The exact role(s) of these channels in the regulation of fluid absorption across gallbladder epithelium will require further examination.

APPENDIX

Intracellular microelectrode studies on epithelial tissues commonly use transepithelial current pulses as a means of estimating the ratio of apical to basolateral membrane resistances (R_a/R_b). Current applied across the epithelium distributes between transcellular and paracellular pathways; the transcellular current (i_c) gives rise to voltage deflections ΔV_{mc} and ΔV_{cs} across the apical and basolateral membranes, respectively. The ratio of the cell membrane resistances is estimated by:

$$\frac{R_a}{R_b} = \frac{\Delta V_{mc}/i_c}{\Delta V_{cs}/i_c} = \frac{\Delta V_{mc}}{\Delta V_{cs}} \tag{A1}$$

In light of the voltage dependence of R_a, we have reexamined the accuracy of $\Delta V_{mc}/\Delta V_{cs}$ as an estimator of R_a/R_b.

In the absence of an applied transepithelial current, the apical and basolateral membrane voltages V_{mc} and V_{cs} can be expressed as follows:

$$V_{mc} = E_a - \frac{(E_a + E_b)\,R_a}{R_a + R_b + R_s} \tag{A2}$$

$$V_{cs} = E_b - \frac{(E_a + E_b)\,R_b}{R_a + R_b + R_s} \tag{A3}$$

where E_a and E_b are the equivalent EMFs of the apical and basolateral membranes (Reuss and Finn, 1975*a*). For convenience, E_a and V_{mc} are referred to the cell interior, while E_b and V_{cs} are referred to the serosal solution. Cable experiments reveal that for tissues bathed in 10 mM HEPES-buffered Ringer's, $E_a = E_b$ (see Table II), so Eqs. A2 and A3 simplify to:

$$V_{mc} = E_a \tag{A4}$$

$$V_{cs} = E_b \tag{A5}$$

Transepithelial serosa-to-mucosa current clamps depolarize V_{mc} and hyperpolarize V_{cs}. Depolarization of V_{mc} activates maxi K^+ channels, reducing R_a to a new value R'_a. As the relative K^+ conductance of the apical membrane increases, E_a shifts to a value E'_a, closer to E_K. Mucosa-to-serosa current clamps have the opposite effects. During a current clamp, the membrane voltages stabilize at values given by:

$$V'_{mc} = E'_a + \left[\frac{i_t R_s - (E'_a + E_b)}{R'_a + R_b + R_s}\right] R'_a \tag{A6}$$

$$V'_{cs} = E_b + \left[\frac{i_b R_s - (E'_a + E_b)}{R'_a + R_b + R_s}\right] R_b \tag{A7}$$

where i_t is the transepithelial current density, deemed positive for mucosa-to-serosa current

clamps. ΔV_{mc} and ΔV_{cs} are obtained by subtracting Eq. A4 from A6, and Eq. A5 from A7. Dividing ΔV_{mc} by ΔV_{cs}:

$$\frac{\Delta V_{mc}}{\Delta V_{cs}} = \frac{(E'_a - E_a) + \left[\frac{i_t R_s - (E'_a + E_b)}{R'_a + R_b + R_s}\right] R'_a}{\left[\frac{i_t R_s - (E'_a + E_b)}{R'_a + R_b + R_s}\right] R_b} \tag{A8}$$

If R_a and E_a are unchanged by the current clamp, then Eq. A8 reduces to R_a/R_b. However, if R_a and E_a do change, then R'_a and E'_a emerge as unknowns, and a second equation relating R'_a and E'_a is required to calculate these two quantities. Recalling that the apical membrane consists to two functionally different channel types—maxi K^+ channels and voltage-independent baseline channels—it follows that the apical membrane EMF at any membrane voltage is given by:

$$E'_a = \left(1 - \frac{R'_a}{R^0_a}\right) E_K + \frac{R'_a}{R^0_a} \tag{A9}$$

where $R'_a = 1/G'_a = 1/(G^0_a + G^K_a)$, and R^0_a and E^0_a are the total resistance and the equilibrium potential of the leakage pathway. For the control case:

$$E_a = \left(1 - \frac{R_a}{R^0_a}\right) E_K + \frac{R_a}{R^0_a} E^0_a \tag{A10}$$

Combining Eqs. A9 and A10 yields:

$$R'_a = R_a \frac{(E'_a - E_K)}{(E_a - E_K)} \tag{A11}$$

Given an experimentally determined value of $\Delta V_{mc}/\Delta V_{cs}$, and the control parameters R_a and E_a from cable analysis experiments, Eqs. A8 and A11 can be used to solve for R'_a (thus G'_a) and E'_a.

We thank K. Dawson for assistance with the microelectrode experiments, G. Altenberg, C. Cotton, S. Lewis, B. Simon, and F. Wehner for comments on a preliminary version of the manuscript, W. Law and J. Chilton for computer-related assistance, and L. Durant for secretarial help.

This research was supported by National Institutes of Health grants DK-38734 and GM-07200.

Original version received 2 May 1989 and accepted version received 27 September 1989.

REFERENCES

Bello-Reuss, E., T. P. Grady, and L. Reuss. 1981. Mechanism of the effect of cyanide on cell membrane potentials in *Necturus* gallbladder epithelium. *Journal of Physiology.* 314:343–357.

Bevington, P. R. 1969. Data Reduction and Error Analysis for the Physical Sciences. McGraw-Hill Book Co., New York. 208–215.

Bjorkman, D. J., C. H. Allan, S. J. Hagen, and J. S. Trier. 1986. Structural features of absorptive cells and microvillus membrane preparations from rat small intestine. *Gastroenterology.* 91:1401–1414.

Blatz, A. L., and K. L. Magleby. 1987. Calcium-activated potassium channels. *Trends in Neurosciences.* 10:463–467.

Bolívar, J. J., and M. Cereijido. 1987. Voltage and Ca^{2+}-activated K^+ channel in cultured epithelial cells (MDCK). *Journal of Membrane Biology.* 97:43–51.

Christensen, O. 1987. Mediation of cell volume regulation by Ca^{2+} influx through stretch-activated channels. *Nature.* 350:66–68.

Christensen, O., and T. Zeuthen. 1987. Maxi K^+ channels in leaky epithelia are regulated by intracellular Ca^{2+}, pH and membrane potential. *Pflügers Archiv.* 408:249–259.

Cook, D. L., M. Ikeuchi, and W. Y. Fujimoto. 1984. Lowering of pH_i inhibits Ca^{2+}-activated K^+ channels in pancreatic B-cells. *Nature.* 311:269–271.

Eisenman, G., R. Latorre, and C. Miller. 1986. Multi-ion conduction and selectivity in the high-conductance Ca^{++}-activated K^+ channel from skeletal muscle. *Biophysical Journal.* 50:1025–1034.

Frindt, G., and L. G. Palmer. 1987. Ca-activated K channels in apical membrane of mammalian CCT, and their role in K secretion. *American Journal of Physiology.* 252:F458–F467.

Frindt, G., and L. G. Palmer. 1989. Low-conductance K channels in apical membrane of rat cortical collecting tubule. *American Journal of Physiology.* 256:F143–F151.

Frömter. E. 1972. The route of passive ion movement through the epithelium of *Necturus* gallbladder. *Journal of Membrane Biology.* 8:259–301.

García-Díaz, J. F., W. Nagel, and A. Essig. 1983. Voltage-dependent K conductance at the apical membrane of *Necturus* gallbladder. *Biophysical Journal.* 43:269–278.

Gögelein, H., and W. Van Driessche. 1981. Noise analysis of the K^+ current through the apical membrane of *Necturus* gallbladder. *Journal of Membrane Biology.* 60:187–198.

Golowasch, J., A. Kirkwood, and C. Miller. 1986. Allosteric effects of Mg^{2+} on the gating of Ca^{2+}-activated K^+ channels from mammalian skeletal muscle. *Journal of Experimental Biology.* 124:5–13.

Grasset, E., P. Gunter-Smith, and S. G. Schultz. 1983. Effects of Na-coupled alanine transport on intracellular K activities and the K conductance of the basolateral membranes of *Necturus* small intestine. *Journal of Membrane Biology.* 71:89–94.

Greger, R., and H. Gögelein. 1987. Role of K^+ conductive pathways in the nephron. *Kidney International.* 31:1055–1064.

Guggino, S. E., W. B. Guggino, N. Green, and B. Sacktor. 1987. Ca^{2+}-activated K^+ channels in cultured medullary thick ascending limb cells. *American Journal of Physiology.* 252:C121–C127.

Gunter-Smith, P. F. 1988. Apical membrane potassium conductance in guinea pig gallbladder epithelial cells. *American Journal of Physiology.* 255:C808–C815.

Hille, B., and W. Schwarz. 1978. Potassium channels as multi-ion single-file pores. *Journal of General Physiology.* 72:409–442.

Hodgkin, A. L., and R. D. Keynes. 1955. The potassium permeability of a giant nerve fibre. *Journal of Physiology.* 128:61–88.

Hunter, M., A. G. Lopes, E. L. Boulpaep, and G. Giebisch. 1984. Single-channel recordings of calcium-activated potassium channels in the apical membrane of rabbit cortical collecting tubules. *Proceedings of the National Academy of Sciences.* 81:4237–4239.

Hunter, M., A. G. Lopes, E. Boulpaep, and G. Giebisch. 1986. Regulation of single potassium ion channels from apical membrane of rabbit collecting tubule. *American Journal of Physiology.* 251:F725–F733.

Kawahara, K., M. Hunter, and G. Giebisch. 1987. Potassium channels in *Necturus* proximal tubule. *American Journal of Physiology.* 253:F488–F494.

Kolb, H. A., C. D. A. Brown, and H. Murer. 1986. Characterization of a Ca-dependent maxi K channel in the apical membrane of a cultured renal epithelium. *Journal of Membrane Biology.* 92:207–215.

Lang, D. G., and A. K. Ritchie. 1987. Large and small conductance calcium-activated potassium channels in the GH3 anterior pituitary cell line. *Pflügers Archiv.* 410:614–622.

Latorre, R. 1986. The large calcium-activated potassium channel. *In* Ion Channel Reconstitution. C. Miller, editor. Plenum Publishing Co., New York. 431–482.

Latorre, R., and C. Miller. 1983. Conduction and selectivity in potassium channels. *Journal of Membrane Biology.* 71:11–30.

Latorre, R., C. Vergara, and C. Hidalgo. 1982. Reconstitution in planar lipid bilayers of a Ca^{2+}-dependent K^+ channel from transverse tubule membranes isolated from rabbit skeletal muscle. *Proceedings of the National Academy of Sciences.* 79:805–809.

Martell, A. E., and R. M. Smith. 1974. Critical Stability Constants, Vol. I. Amino Acids. Plenum Publishing Co., New York. 269.

Maruyama, Y., H. Matsunaga, and T. Hoshi. 1986. Ca^{2+}-and voltage-activated K^+ channel in apical cell membrane of gallbladder epithelium from *Triturus*. *Pflügers Archiv.* 406:563–567.

Marty, A. 1983. Blocking of large unitary calcium-dependent potassium currents by internal sodium ions. *Pflügers Archiv.* 396:179–181.

McManus, O. B., and K. L. Magleby. 1988. Kinetic states and modes of single large-conductance calcium-activated potassium channels in cultured rat skeletal muscle. *Journal of Physiology.* 402:79–120.

Merot, J., M. Bidet, S. LeMaout, M. Tauc, and P. Poujeol. 1989. Two types of K^+ channels in the apical membrane of rabbit proximal tubule in primary culture. *Biochimica et Biophysica Acta.* 978:134–144.

Methfessel, C., and G. Boheim. 1982. The gating of single calcium-dependent potassium channels is described by an activation/blockade mechanism. *Biophysics of Structure and Mechanism.* 9:35–60.

Moczydlowski, E., O. Alvarez, C. Vergara, and R. Latorre. 1985. Effect of phospholipid surface charge on the conductance and gating of a Ca^{2+}-activated K^+ channel in planar lipid bilayers. *Journal of Membrane Biology.* 83:273–282.

Moczydlowski, E., and R. Latorre. 1983. Gating kinetics of Ca^{2+}-activated K^+ channels from rat muscle incorporated into planar lipid bilayers. Evidence for two voltage-dependent Ca^{2+} binding reactions. *Journal of General Physiology.* 82:511–542.

Montrose, M. H., R. Lester, P. Zimniak, M. S. Anwer, and H. Murer. 1988. Bile acids increase cellular free calcium in cultured kidney cells (LLC-PK_1). *Pflügers Archiv.* 412:164–171.

Morris, A. P., D. V. Gallacher, and J. A. C. Lee. 1986. A large conductance, voltage- and calcium-activated K^+ channel in the basolateral membrane of rat enterocytes. *FEBS Letters.* 206:87–92.

Neyton, J., and C. Miller. 1988. Discrete Ba^{2+} block as a probe of ion occupancy and pore structure in the high-conductance Ca^{2+}-activated K^+ channel. *Journal of General Physiology.* 92:569–586.

Palant, C. E., and I. Kurtz. 1987. Measurement of intracellular Ca^{2+} activity in *Necturus* gallbladder. *American Journal of Physiology.* 253:C309–C315.

Pallotta, B. S. 1985. Calcium-activated potassium channels in rat muscle inactivate from a short-duration open time. *Journal of Physiology.* 363:501–516.

Pallotta, B. S., J. R. Helper, S. A. Ogelsby, and T. K. Harden. 1987. A comparison of calcium-activated potassium channel currents in cell-attached and excised patches. *Journal of General Physiology.* 89:985–998.

Palmer, L. G. 1986. Patch-clamp technique in renal physiology. *American Journal of Physiology.* 19:F379–F385.

Parent, L., J. Cardinal, and R. Sauve. 1988. Single-channel analysis of a K channel at basolateral membrane of rabbit proximal convoluted tubule. *American Journal of Physiology.* 254:F105–F113.

Petersen, K.-U., and L. Reuss. 1983. Cyclic AMP-induced chloride permeability in the apical membrane of *Necturus* gallbladder epithelium. *Journal of General Physiology.* 81:705–729.

Reinhart, P. H., S. Chung, and I. B. Levitan. 1989. A family of calcium-dependent potassium channels from rat brain. *Neuron.* 2:1031–1041.

Reuss, L. 1981. Potassium transport mechanisms by amphibian gallbladder. *In* Ion Transport by Epithelia. S. G. Schultz, editor. Raven Press, New York, 109–128

Reuss, L. 1989. Ion transport across gallbladder epithelium. *Physiological Reviews.* 69:503–545.

Reuss, L., L. Y. Cheung, and T. P. Grady. 1981. Mechanisms of cation permeation across apical cell membrane of *Necturus* gallbladder: effects of luminal pH and divalent cations on K^+ and Na^+ permeability. *Journal of Membrane Biology.* 59:211–224.

Reuss, L., and A. L. Finn. 1975*a*. Electrical properties of the cellular transepithelial pathways in *Necturus* gallbladder. I. Circuit analysis and steady-state effects of mucosal solution substitutions. *Journal of Membrane Biology.* 25:115–139.

Reuss, L., and A. L. Finn. 1975*b*. Electrical properties of the cellular transepithelial pathway in *Necturus* gallbladder. II. Ionic permeability of the apical cell membrane. *Journal of Membrane Physiology.* 25:141–161.

Sackin, H., and L. G. Palmer. 1987. Basolateral potassium channels in renal proximal tubule. *American Journal of Physiology.* 253:F476–F487.

Sakmann, B., and E. Neher. 1983. Geometric parameters of pipettes and membrane patches. *In* Single-Channel Recording. B. Sakmann and E. Neher, editors. Plenum Publishing Co., New York. 37–52.

Segal, Y., and L. Reuss. 1988. Large-conductance K^+ channels in *Necturus* gallbladder epithelium. *Journal of General Physiology.* 94:34*a* (Abstr.)

Segal, Y., and L. Reuss. 1989. Cl^- channels in cyclic AMP-stimulated gallbladder epithelium. *FASEB Journal.* 3:A862. (Abstr.)

Segal, Y., and L. Reuss. 1990. Effects of Ba^{2+}, TEA^+ and quinine on apical membrane K^+ conductance and Maxi K^+ channels in *Necturus* gallbladder epithelium. *American Journal of Physiology.* In press.

Sheppard, D. N., F. Giraldez, and F. V. Sepúlveda. 1988. Kinetics of voltage-and Ca^{2+}-activation and Ba^{2+} blockade of a large conductance K^+ channel from *Necturus* enterocytes. *Journal of Membrane Biology.* 105:65–75.

Singer, J. J., and J. V. Walsh, Jr. 1987. Characteristics of calcium-activated potassium channels in single smooth muscle cells using the patch-clamp technique. *Pflügers Archiv.* 408:98–111.

Stoddard, J., and L. Reuss. 1988*a*. Dependence of cell membrane conductances on bathing solution (HCO_3^-/CO_2 in *Necturus* gallbladder. *Journal of Membrane Biology.* 102:163–174.

Stoddard, J., and L. Reuss. 1988*b*. Voltage- and time-dependence of apical membrane conductance during current clamp in *Necturus* gallbladder epithelium. *Journal of Membrane Biology.* 103:191–204.

Tsien, R. Y., and T. J. Rink. 1980. Neutral carrier ion-selective microelectrodes for measurement of intracellular free calcium. *Biochimica et Biophysica Acta.* 599:623–638.

Vergara, C., and R. Latorre. 1983. Kinetics of Ca^{2+}-activated K^+ channels from rabbit muscle incorporated into planar bilayers. Evidence for a Ca^{2+} and Ba^{2+} blockade. *Journal of General Physiology.* 82:543–568.

Weinman, S. A., and L. Reuss. 1982. Na^+-H^+ exchange at the apical membrane of *Necturus* gallbladder. Extracellular and intracellular pH studies. *Journal of General Physiology.* 80:299–321.

Wills, N. K., and A. Zweifach. 1987. Recent advances in the characterization of epithelial ionic channels. *Biochimica et Biophysica Acta.* 906:1–31.

Ziomek, C. A., S. Schulman, and M. Edidin. 1980. Redistribution of membrane proteins in isolated mouse intestinal epithelial cells. *Journal of Cell Biology.* 86:849–857.